

Identification of Histone Peptide Binding Specificity and Small-Molecule Ligands for the TRIM33 α and TRIM33 β Bromodomains

Published as part of the ACS Chemical Biology special issue “Epigenetics 2022”.

Angelina R. Sekirnik,[‡] Jessica K. Reynolds,[‡] Larissa See, Joseph P. Bluck, Amy R. Scorch, Cynthia Tallant, Bernadette Lee, Katarzyna B. Leszczynska, Rachel L. Grimley, R. Ian Storer, Marta Malattia, Sara Crespillo, Sofia Caria, Stephanie Duclos, Ester M. Hammond, Stefan Knapp, Garrett M. Morris, Fernanda Duarte, Philip C. Biggin, and Stuart J. Conway*



Cite This: *ACS Chem. Biol.* 2022, 17, 2753–2768



Read Online

ACCESS |



Metrics & More

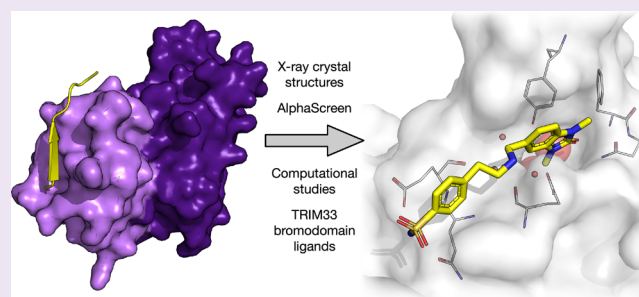


Article Recommendations



Supporting Information

ABSTRACT: TRIM33 is a member of the tripartite motif (TRIM) family of proteins, some of which possess E3 ligase activity and are involved in the ubiquitin-dependent degradation of proteins. Four of the TRIM family proteins, TRIM24 (TIF1 α), TRIM28 (TIF1 β), TRIM33 (TIF1 γ) and TRIM66, contain C-terminal plant homeodomain (PHD) and bromodomain (BRD) modules, which bind to methylated lysine (KMe_n) and acetylated lysine (KAc), respectively. Here we investigate the differences between the two isoforms of TRIM33, TRIM33 α and TRIM33 β , using structural and biophysical approaches. We show that the N1039 residue, which is equivalent to N140 in BRD4(1) and which is conserved in most BRDs, has a different orientation in each isoform. In TRIM33 β , this residue coordinates KAc, but this is not the case in TRIM33 α . Despite these differences, both isoforms show similar affinities for H3_{1–27}K18Ac, and bind preferentially to H3_{1–27}K9Me₃K18Ac. We used this information to develop an AlphaScreen assay, with which we have identified four new ligands for the TRIM33 PHD-BRD cassette. These findings provide fundamental new information regarding which histone marks are recognized by both isoforms of TRIM33 and suggest starting points for the development of chemical probes to investigate the cellular function of TRIM33.



INTRODUCTION

TRIM33 is a member of the tripartite motif (TRIM) family of proteins, which are characterized by an N-terminal tripartite motif typically containing one RING-finger domain, one or two zinc-finger domains (B1 box and B2 box), and an associated coiled-coil region. Most TRIM proteins possess E3 ligase activity and are involved in the ubiquitin-dependent degradation of a number of important proteins.^{1,2} Four of the TRIM family proteins, TRIM24 (TIF1 α), TRIM28 (TIF1 β), TRIM33 (TIF1 γ), and TRIM66, possess C-terminal plant homeodomain (PHD) and bromodomain (BRD) modules (Figure 1A–C), which bind to methylated lysine (KMe_n) and acetylated lysine (KAc), respectively.

PHDs are small, independently folded, 50–80 residue long protein domains. Over 170 sequences have been annotated as PHD fingers in the human genome.³ They contain conserved regions of cysteine and histidine residues that coordinate two Zn²⁺ ions in a cross braced fashion, with an antiparallel two-stranded β -sheet core, which imposes conformational stability.^{3–7} These domains read a range of histone marks, notably the methylation state of the K4 residue of H3 histone

(H3K4Me₃, H3K4Me₂, or H3K4Me₀) and the H3K9 and H3R2 positions.^{8,9} Mutations within this motif have been linked to immunological, neurological, and developmental disorders.^{9,10}

BRDs are well characterized protein modules comprising approximately 110 amino acids that bind to KAc residues on histones and many other proteins.^{11–15} Their well-defined tertiary structure comprises a left-handed, antiparallel four-helical bundle (α A, α B, α C, and α Z),¹⁶ which is structurally conserved across the family, despite relatively low sequence identity.¹⁷ The KAc binding pocket of most BRDs is hydrophobic but contains structural water molecules at the base of the pocket and, in some cases, in the ZA channel.¹⁸ The ability of these water molecules to be displaced varies

Received: March 28, 2022

Accepted: August 30, 2022

Published: September 13, 2022



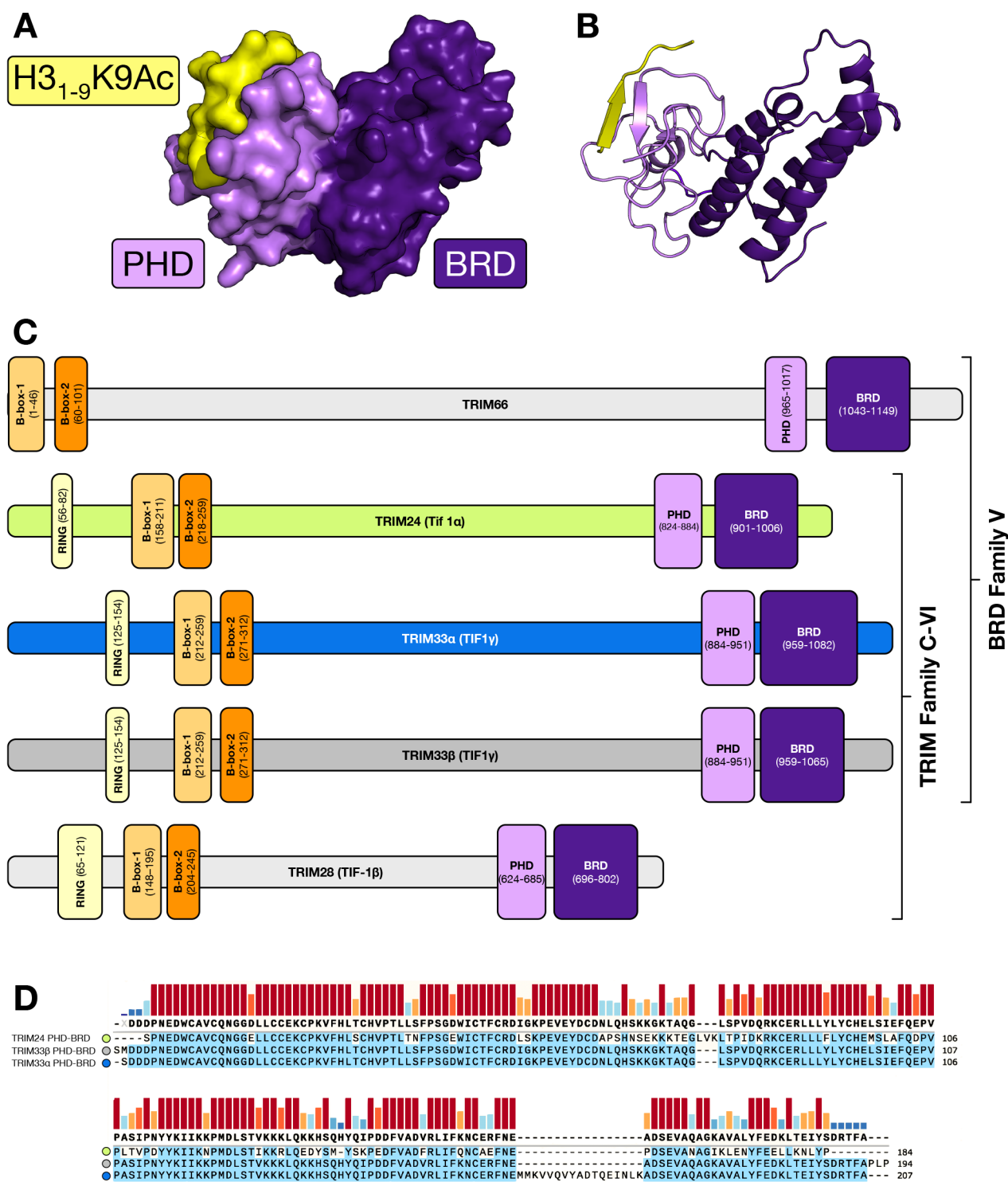


Figure 1. X-ray crystal structure of the PHD-BRD cassette of TRIM33 β bound to H3₁₋₉K9Ac (PDB code 5MR8) with (A) the surface represented and (B) the cartoon showing the extended β -sheet formed between the PHD and H3₁₋₉K9Ac. Figures were generated using the PyMOL Molecular Graphics System, version 2.5, Schrödinger, LLC. (C) Domain composition of TRIM24, TRIM28, TRIM33, and TRIM66. The PHD (lilac) and BRD (purple) domains of TRIM proteins sit at the C-terminus of the proteins. The TRIM family C–VI proteins (TRIM24, TRIM28, and TRIM33) and the homologous TRIM66 possess a tandem PHD-BRD cassette. TRIM24, TRIM33, and TRIM66 are in BRD Family V. Figure generated using OmniGraffle. (D) TRIM24 PHD-BRD has 62.0% identity and 75.5% similarity with TRIM33 α . TRIM24 PHD-BRD has 67.8% identity and 82.5% similarity with TRIM33 β . TRIM33 α has 91.8% identity and 91.8% similarity with TRIM33 β ; they are identical apart from the 17 amino acid insertion/deletion. The primary sequences were obtained from PDB files 3U5O (TRIM33 α), 4YC9 (TRIM24), and 5MR8 (TRIM33 β). Local alignment is Smith–Waterman using SnapGene.

between classes of BRDs and has been exploited to develop selective ligands for certain proteins.^{19,20} The canonical BRDs possess a highly conserved asparagine residue, which forms a hydrogen bond to KAc. However, 13 non-canonical BRDs exist, 12 of which possess threonine or tyrosine residues at this position that are, in principle, capable of hydrogen-bonding to KAc.¹⁵ One of these is TRIM28, in which the asparagine residue is replaced by a threonine.¹⁵ In addition, the 17-amino acid insertion in TRIM33 α (see below) moves this asparagine out of the KAc-binding pocket, resulting in no obvious residue that can interact with KAc at this position. The inherent affinity of BRDs for a single KAc amino acid is low, and further affinity is derived from interactions with the cognate peptide/protein, which also confers selectivity for given acetylated binding partners.²¹ These PHD and BRD modules enable chromatin binding of proteins, and consistent with this, deletion of either the BRD or the PHD in TRIM33 prevents its localization to sites of DNA breaks.²²

The biological functions of TRIM24, TRIM28, TRIM33, and TRIM66 have been investigated, and some key findings are briefly described below. Overexpression of TRIM24 is connected to tumor progression and poor prognosis in breast cancer,²³ and significant upregulation has been observed in cancers including gastric cancer,²⁴ non-small-cell lung cancer,²⁵ leukemia,²⁶ prostate cancer,²⁷ and hepatocellular carcinoma.²⁸ Knockdown of TRIM24 in colon cancer cell lines suppressed tumor growth and induced apoptosis.²⁹ Despite mouse models indicating that TRIM24 can act as a liver-specific tumor suppressor,³⁰ most studies show that TRIM24 is an oncogene when overexpressed.

TRIM33 is a tumor suppressor in breast cancer,³¹ non-small-cell lung cancer,³² and clear cell renal cell carcinoma³³ and, through its role in β -catenin degradation, prevents brain tumor development and human glioblastoma.³⁴ TRIM33 also has a role in regulation of the transforming growth factor beta (TGF- β) superfamily.^{35,36} In contrast, TRIM33 can also function as a tumor promoter by preventing apoptosis in B lymphoblastic leukemia,³⁷ demonstrating that TRIM33 has a range of biological functions.³⁸ TRIM33 also plays a role in the poly(ADP-ribose) polymerase (PARP)-dependent DNA damage response pathway.²² TRIM66 has also recently been shown to act in the DNA damage response and binds to H3R2K4 and H3K56Ac.³⁹ Prior to their identification,⁴⁰ biological studies did not distinguish between the two TRIM33 isoforms, TRIM33 α and TRIM33 β .

The location of two reader domains proximal to each other in TRIM24, TRIM28, TRIM33, and TRIM66 raised the question of whether and how these domains function together. It is possible that binding of a target protein to one domain will result in a different biological response to binding to the other domain or both domains simultaneously.

The H3 histone modifications recognized by TRIM24, TRIM28, TRIM33, and TRIM66 have been the subject of a number of studies. The targets of the TRIM24 reader domains were identified by Tsai et al., reporting TRIM24 as a dual reader of unmodified H3K4 and H3K23Ac.²³ Xi et al. have characterized TRIM33 α , the full-length isoform of TRIM33. The PHD of TRIM33 α binds to unmodified H3K4 and H3K9Me₃ through an interaction with W889.³⁶ This residue is conserved in TRIM24, where binding to H3K9Me₃ has been reported but not quantified.⁴¹ The BRD of TRIM33 α binds to H3K18Ac, which is an appropriate distance from H3K9 to be read simultaneously. A recent study by Chen et al.

demonstrated that all peptides binding to the PHD of TRIM24, TRIM33, or TRIM66 require unmodified H3R2.³⁹

The study by Xi et al. focused on the TRIM33 α isoform, which contains a BRD with a 17-amino acid insertion on the BC loop, compared to the TRIM24 sequence.³⁶ However, a second isoform of TRIM33 has been identified, TRIM33 β ,⁴⁰ which is a splice variant that lacks the 17-amino acid insertion and is homologous to TRIM24 (Figure 1D). The histone H3 binding profile of TRIM33 β has not previously been compared to TRIM33 α , and the role of the extended BC loop in TRIM33 α has not been explored. The X-ray crystal structures of TRIM33 α show a non-canonical BRD, in which the conserved N1039 residue is located outside of the KAc-binding pocket, indicating that it cannot interact with KAc,³⁶ and no residue replaces N1039 to compensate. Additionally, prior to this work there was no structural information on the TRIM33 β isoform to demonstrate the location of the N1039 residue.

Over the past decade, BRDs have emerged as a ligandable class of protein modules that are therapeutically relevant.^{12,13,18,42–45} Despite this, the TRIM proteins remain among the most understudied BRD-containing targets. Ligands for the BRD of TRIM24, which also bind to the BRD of BRPF1, have been reported by both Palmer et al.^{46,47} and Bennett et al.⁴⁸ In addition, a PROTAC for TRIM24 was developed and confirmed TRIM24 as a novel dependency in acute leukemia.²⁶ At the start of this work, there were no reported small molecule ligands for either isoform of TRIM33. In a recent patent, multiple putative TRIM33 α ligands were disclosed;⁴⁹ there are no non-peptide ligands reported for the PHDs of TRIM24 or TRIM33.

Here we report an analysis of the histone H3 peptide binding profile of TRIM24, TRIM33 α , and TRIM33 β . We show that both TRIM33 α and TRIM33 β bind preferentially to H3_{1–27}K9Me₃K18Ac. Surprisingly, we found that TRIM33 α and TRIM33 β have similar binding affinities for H3_{1–27}K18Ac, despite the non-canonical BRD of TRIM33 α . We also show that the PHD and BRD of these proteins contribute equally to the affinity for the dual modified H3_{1–27}K9Me₃K18Ac peptide and that this contribution is additive. We have employed this information to develop an AlphaScreen assay^{50,51} for the tandem PHD-BRD cassettes of TRIM24, TRIM33 α , and TRIM33 β . Using these assays, we screened approximately 1700 compounds, and identified novel ligands for TRIM24, TRIM33 α , and TRIM33 β . We also show that the compounds disclosed in a recent patent⁴⁹ do not bind to TRIM33 β in our hands. This work provides the foundation for the development of more refined TRIM33 ligands, which will enable the function of this fascinating protein to be further explored and potentially recruited as an E3 ligase in proteolysis-targeting chimeras (PROTACs).

RESULTS AND DISCUSSION

TRIM33 Has Higher Expression Levels in Cancer Cell Lines Compared to Noncancer Cell Lines. To determine whether TRIM33 is of potential interest as a therapeutic target in oncology, we compared the expression levels of TRIM33 in a range of cancer and noncancer cell lines using Western blotting (Figure 2). We demonstrate that the cancer cell lines generally show higher expression levels of both TRIM33 and amplified in liver cancer 1 (ALC1 or CHD1L) compared to related noncancer cell lines. ALC1 is a helicase that is recruited to the site of single strand breaks (SSBs) through binding of its macrodomain to poly(ADP-ribose) (PAR). Its helicase activity

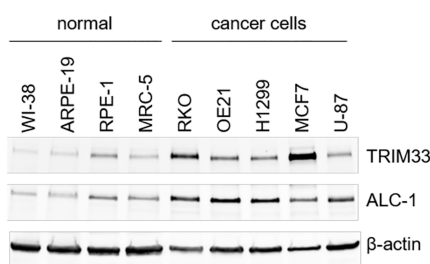


Figure 2. Western blot analysis of expression levels in cancer and noncancer cell lines show that both TRIM33 and amplified in liver cancer 1 (ALC1 or CHD1L) are generally present in higher levels in the cancer cell lines. Noncancerous cell lines: WI-38 = lung fibroblasts; ARPE-19 = retinal pigment epithelial cells; RPE-1 = retinal pigment epithelial cells; MRC-5 = lung. Cancer cell lines: RKO = colon carcinoma; OE21 = esophageal squamous cell carcinoma; H1299 = non-small-cell lung carcinoma; MCF7 = breast adenocarcinoma; U-87 = glioblastoma.

relaxes the chromatin structure to allow repair, but this activity is short-lived ($t_{1/2} \approx 2.5$ min) and tightly regulated as prolonged chromatin relaxation exposes it to further damage.⁵² TRIM33 is recruited to the site of SSBs in an ALC1-dependent manner and is required to ensure timely dissociation of ALC1 from chromatin.²² TRIM33 does not bind PAR directly, but deletion of the chromatin-binding PHD/BRD module prevents TRIM33 localization to sites of laser scissor-induced DNA breaks. TRIM33 (sh/siRNA) knock down studies conducted by Kulkarni et al.²² showed accumulation of ALC1 at the sites of DNA damage, evidence of DNA damage-induced checkpoint activation, and prolonged DNA damage. Combined with our data, these observations raise the possibility that inhibition of TRIM33 BRD or PHD function or both might be of therapeutic benefit in cancers that have high levels of TRIM33. These data encouraged us to identify ligands for the TRIM33 BRD and PHD to probe their functions.

TRIM33 β Contains a Canonical Bromodomain. We were interested to investigate the effect of the 17-amino acid deletion observed in TRIM33 β on its BRD structure, and whether this alteration affected the orientation of N1039 in

relation to the KAc binding pocket. To achieve this, we sought to obtain X-ray crystal structures of the TRIM33 β BRD and PHD cassette, as X-ray structural data have only previously been reported for TRIM33 α . The TRIM33 β cassette (residues 888–1127) was expressed and cocrystallized with the PHD-binding region of the H3 peptide (H3_{1–9}K9Ac) (PDB 5MR8). We also obtained an X-ray crystal structure of 7ZDD construct bound to a peptide that does not occur naturally, H3_{1–10}K10Ac, which possesses the first 9 residues of the H3 peptide (K9 unmodified) with a KAc residue added as the 10th residue. This peptide was ordered in error, but the X-ray crystal structure with it bound still provides useful structural information and so we have included it here. Both 5MR8 and 7ZDD show the TRIM33 β PHD-BRD cassette crystallizing with the H3-mimicking peptide bound to the PHD of one protein chain, through residues 1–8, with the K9Ac or K10Ac residue occupying the KAc binding pocket of an adjacent protein chain (Figure 3A,B).

Both X-ray crystal structures show that the BRD of TRIM33 β is canonical, with N1039 residing inside the KAc-binding pocket, unlike TRIM33 α (Figure 4A), where the residue is located 6.2 Å away (N1039 NH₂ to NH₂ distance) outside of the pocket. The H3-mimicking peptides form very similar interactions with TRIM33 β to those formed with TRIM33 α (Figure 4B–D). The peptide acts as an extended β -sheet, with a significant number of backbone interactions observed. The necessity of unmodified H3R2 for effective binding is reflected by this residue forming interactions with a number of residues; the interaction with N886 is present in all structures. The same is true for unmodified H3K4, which interacts with D884, E887, D888, and the backbone carbonyl oxygen of N886. H3N5 hydrogen bonds to D898, and H3R8 forms interactions with H910 (Figure 4B–D). The KAc residues do not form any interactions with the protein in *cis* (i.e., to the same protein), as they are bound to the BRD of an adjacent protein copy in *trans* (see above).

The TRIM33 β PHD-BRD Domains Bind to Histone H3 K9Me₃ and K18Ac Marks. To establish an AlphaScreen assay,^{13,50,51} the PHD-BRD cassettes of TRIM24 and both TRIM33 isoforms were expressed with an N-terminal His₆ tag

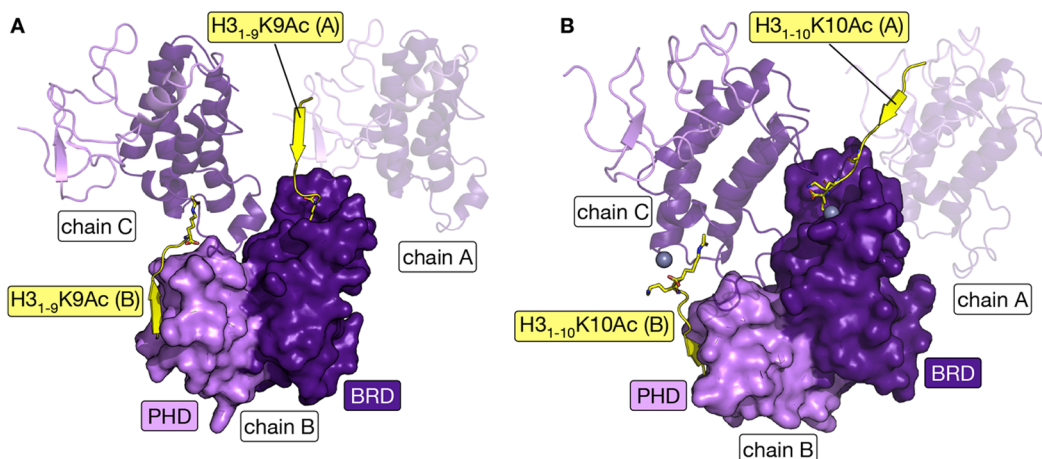


Figure 3. X-ray crystal structures of TRIM33 β bound to (A) H3_{1–9}K9Ac (PDB code 5MR8) or (B) H3_{1–10}K10Ac (PDB code 7ZDD). Two symmetry mates are shown (represented as cartoon) revealing that, in both cases, the H3-mimicking peptide binds to the PHD of one chain and the KAc-binding pocket of an adjacent protein (i.e., in *trans*). Figures generated using the PyMOL Molecular Graphics System, version 2.5, Schrödinger, LLC.

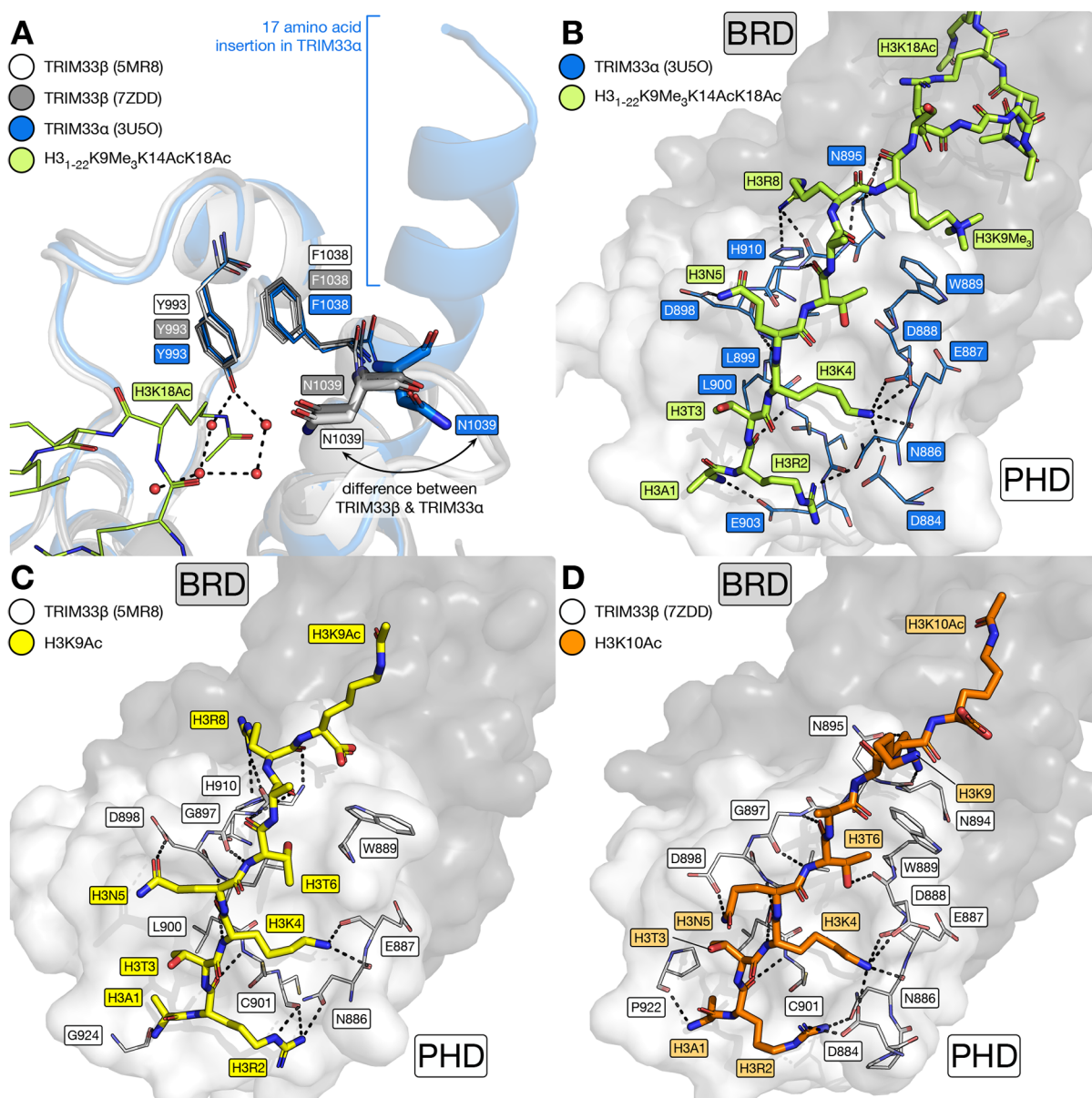


Figure 4. X-ray crystal structures of the TRIM33 α and - β BRD and PHD cassettes. (A) Overlay of the X-ray crystal structures of the TRIM33 α BRD-PHD (carbon = blue, PDB code 3U5O) in complex with the histone H3-mimicking peptide H₃₁₋₂₂K9Me₃K14AcK18Ac (carbon = lime, PDB code 3U5O),³⁶ and the TRIM33 β PHD-BRD (PDB codes 5MR8 and 7ZDD). Both X-ray crystal structures of TRIM33 β show that the BRD is canonical, with N1039 residing inside the KAc-binding pocket, while this residue sits outside of the pocket in TRIM33 α . The 17 amino acid extension present in TRIM33 α is shown as a blue helix cartoon. (B) H₃₁₋₂₂K9Me₃K14AcK18Ac (carbon = lime, PDB code 3U5O) peptide forms a number of backbone interactions resulting in an extended β -sheet structure with the PHD of TRIM33 α (carbon = blue, PDB code 3U5O). H3R2 interacts with N886 and H3K4 forms interactions with D884, E887, D888, and the backbone carbonyl oxygen of N886. The side chains of H3N5 and H3R8 also interact with the TRIM33 α PHD. H3K9Me₃ is observed in proximity to W889, implying the existence of a cation- π interaction. Both the H₃₁₋₉K9Ac (C; carbon = yellow) and H₃₁₋₁₀K10Ac (D; carbon = orange) peptides form similar interactions with the TRIM33 β PHD to those formed by H₃₁₋₂₂K9Me₃K14AcK18Ac with the TRIM33 α PHD. Figures generated using the PyMOL Molecular Graphics System, version 2.5, Schrödinger, LLC.

attached (CD spectra for these constructs are shown in Figure S9). Consistent with the X-ray crystallography data above, it has been established previously that methylation of the K4 position of histone H3 reduces affinity to the PHD finger: K_d values for the TRIM24 PHD have been measured by ITC as 8.6 μ M for H₃₁₋₁₅K4Me₀, 41 μ M for H₃₁₋₁₅K4Me₁, 198 μ M for H₃₁₋₁₅K4Me₂, and >400 μ M for H₃₁₋₁₅K4Me₃.⁵³ The presence of the four N-terminal residues of the peptide (H₃₁₋₄), which are recognized by the β -sheet surface of the

PHD finger, are essential for affinity to TRIM33 α .³⁵ Consequently, we maintained K4Me₀ in most of the peptides investigated, to avoid affinities falling below detection limits. The peptide recognition profiles of TRIM24, TRIM33 α , and TRIM33 β were investigated by determining affinity of their tandem BRD-PHD cassettes for H3-mimicking peptides containing combinations of acetylation at K14, K18, or K23, and methylation of K9 (Table 1).

Table 1. AlphaScreen IC₅₀ Values for Modified Histone H3-Based Peptides Binding to the PHD-BRD Cassette of TRIM24, TRIM33 α , or TRIM33 β ^a

Peptide	TRIM24 PHD-BRD IC ₅₀ (μ M) (AlphaScreen)	TRIM33 α PHD-BRD IC ₅₀ (μ M) (AlphaScreen)	TRIM33 β PHD-BRD IC ₅₀ (μ M) (AlphaScreen)
H3 ₁₋₂₇ K14Ac	59.1 \pm 18.6	87.2 \pm 8.05	161 \pm 18.1
H3 ₅₋₂₄ K14Ac	47.4 \pm 2.89	no binding	103 \pm 5.49
H3 ₁₋₂₇ K18Ac	3.51 \pm 0.629	1.22 \pm 0.160	0.959 \pm 0.041
H3 ₁₋₂₇ K23Ac	0.182 \pm 0.012	106 \pm 10.7	9.66 \pm 1.76
H3 ₁₋₂₇ K9Me ₃	0.590 \pm 0.045	2.22 \pm 0.633	1.11 \pm 0.119
H3 ₁₋₂₇ K9Me ₃ K18Ac	0.0789 \pm 0.002	0.778 \pm 0.059	0.620 \pm 0.038
H3 ₁₋₂₇ K9Me ₃ K23Ac	0.149 \pm 0.004	28.4 \pm 2.82	94.9 \pm 18.9
H3 ₁₋₂₇ K18AcK23Ac	0.0768 \pm 0.002	7.92 \pm 1.24	8.00 \pm 1.13
H3 ₁₋₂₇ K9Me ₃ K18AcK23Ac	0.0425 \pm 0.001	10.7 \pm 1.64	1.46 \pm 0.067
H3 ₁₋₂₇	19.8 \pm 2.60	96.8 \pm 4.75	119 \pm 9.49

^aDose-response of unbiotinylated peptide displacing the biotinylated equivalent from the protein. Values quoted are the mean of triplicate data \pm standard error of the mean. A heatmap display is used with “hot” colors corresponding to lower K_d values. See Tables S14 and S15 for peptide concentration and sequences.

Table 2. ITC K_d Values for Modified Histone H3-Based Peptides Binding to the PHD-BRD Cassette of TRIM24, TRIM33 α , or TRIM33 β ^a

Peptide	TRIM24 PHD-BRD K _d (μ M) (ITC)	TRIM33 α PHD-BRD K _d (μ M) (ITC)	TRIM33 β PHD-BRD K _d (μ M) (ITC)
H3 ₁₋₂₇ K9Me ₃	3.90 \pm 0.423 μ M	11.2 \pm 0.760 μ M	9.81 \pm 2.33 μ M
H3 ₁₋₂₇ K18Ac	4.37 \pm 0.430 μ M	10.0 \pm 0.319 μ M	8.95 \pm 0.643 μ M
H3 ₁₋₂₇ K9Me ₃ K18Ac	1.94 \pm 0.111 μ M	9.28 \pm 0.214 μ M	4.78 \pm 0.200 μ M

^aValues quoted from a representative run \pm error of the curve fit. H3-peptide was injected (20 \times 2 μ L injections) into a cell containing protein in 50 mM HEPES buffer, pH 7.4, 150 mM NaCl. Raw heat effects for the data are shown in the Supporting Information. A heatmap display is used with “hot” colors corresponding to lower K_d values.

Table 3. AlphaScreen Signal Response for Biotinylated Peptides with Proteins Bearing Inactive Mutations^a

Peptide	TRIM24 PHD-BRD (% activity)				TRIM33 α PHD-BRD (% activity)			TRIM33 β PHD-BRD (% activity)		
	WT	W828A	N980A	N980F	WT	W889A	N1039F	WT	W889A	N1039F
H3 ₁₋₂₇ K9Me ₃	100	0.74	84	61	100	2.1	98	100	1.2	46
H3 ₁₋₂₇ K18Ac	100	72	43	4.1	100	20	99	100	81	14
H3 ₁₋₂₇ K9Me ₃ K18Ac	100	65	72	33	100	36	96	100	86	58

^aPeptides were serially diluted 1:2. A heatmap display is used, with high percentage activity shown in red and low percentage activity shown in green. High percentage activity indicates binding of the peptide to the protein; reduced percentage activity indicates reduced binding. Percentage activity was calculated using the equation shown in the Supporting Information. Binding curves generated using GraphPad Prism are shown in the Supporting Information.

The data from the AlphaScreen assay show that the TRIM24 PHD-BRD binds preferentially to H3₁₋₂₇K23Ac over the other monoacetylated peptides, while both TRIM33 α and TRIM33 β PHD-BRD bind preferentially to H3₁₋₂₇K18Ac, which is consistent with the literature (Table 1).^{36,53} We note that the dual modified peptide H3₁₋₂₇K18AcK23Ac shows increased affinity for the TRIM24 PHD-BRD (IC₅₀ = 0.0768 \pm 0.002 μ M vs 0.182 \pm 0.012 μ M for H3₁₋₂₇K18Ac).

Conversely, H3₁₋₂₇K18AcK23Ac has lower affinity for both TRIM33 α (IC₅₀ = 7.92 \pm 1.24 μ M vs 1.22 \pm 0.160 μ M for H3₁₋₂₇K18Ac) and TRIM33 β (IC₅₀ = 8.00 \pm 1.13 vs 0.959 \pm 0.041 μ M for H3₁₋₂₇K18Ac) PHD-BRD. It is interesting that the TRIM33 α PHD-BRD and TRIM33 β PHD-BRD show the same affinity for H3₁₋₂₇K18Ac, despite the difference in orientation of N1039 in these constructs.

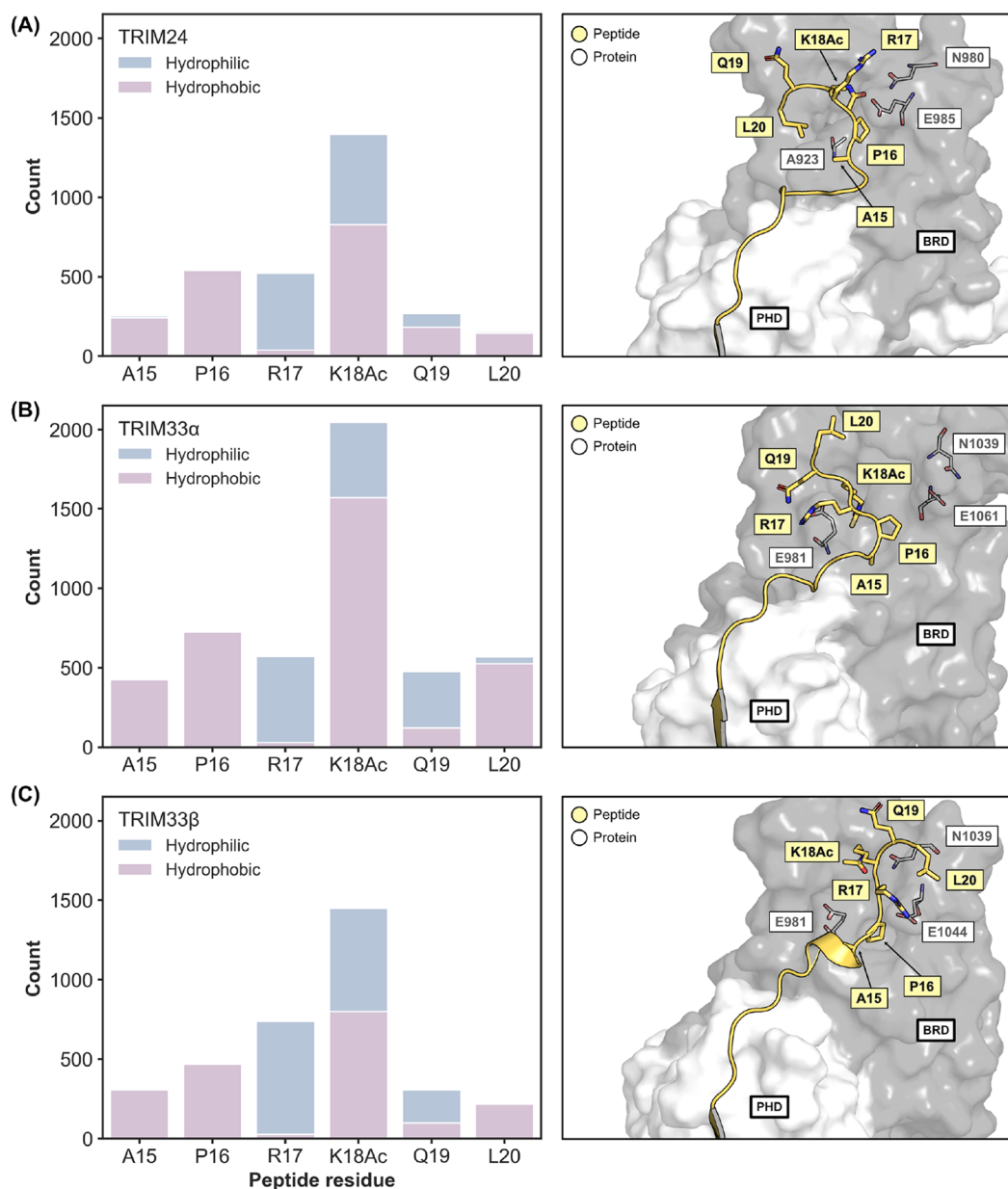


Figure 5. Hydrophobic and hydrophilic contact analysis for (A) TRIM24, (B) TRIM33 α , and (C) TRIM33 β , showing that H3K18Ac forms more interactions with the BRDs as compared to other peptide residues. Protein–Ligand Interaction Profiler (PLIP) was run on 101 frames, taken 1 ns apart, from each of the 5 independent MD runs, totalling 505 frames for each protein. Beside each bar plot a representative snapshot of the peptide bound to each BRD is shown, which corresponds to the middle structure of the top cluster based on the root-mean-squared deviation (RMSD) of the backbone atoms of peptide residues 15–20. The images of the proteins were made using the PyMOL Molecular Graphics System, version 2.5, Schrödinger, LLC.

All three proteins bind to H3_{1–27}K9Me₃, with the TRIM24 PHD–BRD showing approximately double the affinity ($IC_{50} = 0.590 \pm 0.045 \mu M$) compared to the TRIM33 α ($IC_{50} = 2.22 \pm 0.633 \mu M$) or TRIM33 β PHD–BRD ($IC_{50} = 1.11 \pm 0.119 \mu M$). Despite their different sequence preferences for the monoacetylated peptides, all three constructs show preferential binding to the dual modified H3_{1–27}K9Me₃K18Ac peptide, compared to H3_{1–27}K9Me₃K23Ac peptide (Table 1). The structural data indicate that K9Me₃ and K18Ac are optimally spaced to allow simultaneous binding to the PHD and BRD in *cis*, resulting in higher affinity compared to H3_{1–27}K9Me₃K23Ac. The TRIM33 α and TRIM33 β PHD–BRD have the highest affinity for the H3_{1–27}K9Me₃K18Ac

peptide; additional modifications to the peptide all result in reduced affinity. Interestingly, the dual modified H3_{1–27}K18AcK23Ac peptide shows similar affinity ($IC_{50} = 0.0768 \pm 0.002 \mu M$) for the TRIM24 PHD–BRD to the H3_{1–27}K9Me₃K18Ac peptide ($IC_{50} = 0.0789 \pm 0.002 \mu M$). The TRIM24 PHD–BRD shows the highest affinity for the H3_{1–27}K9Me₃K18AcK23Ac peptide ($IC_{50} = 0.0425 \pm 0.001 \mu M$).

To confirm the data obtained using our AlphaScreen assay, we investigated the affinity of the H3_{1–27}K9Me₃, H3_{1–27}K18Ac, and H3_{1–27}K9Me₃K18Ac peptides for the TRIM24, TRIM33 α , and TRIM33 β PHD–BRD using ITC (Table 2). The data obtained show similar trends to the AlphaScreen data. The

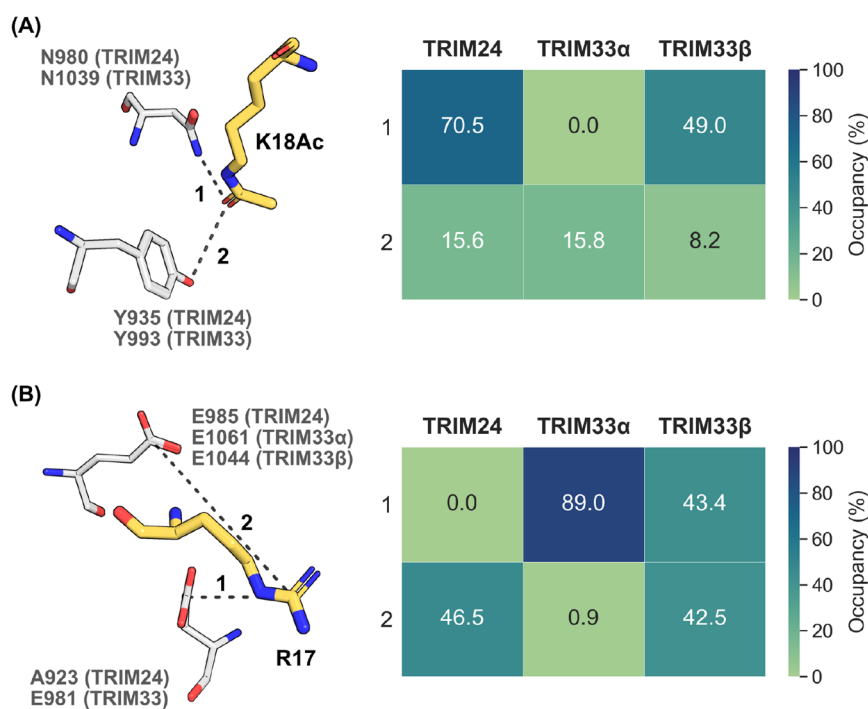
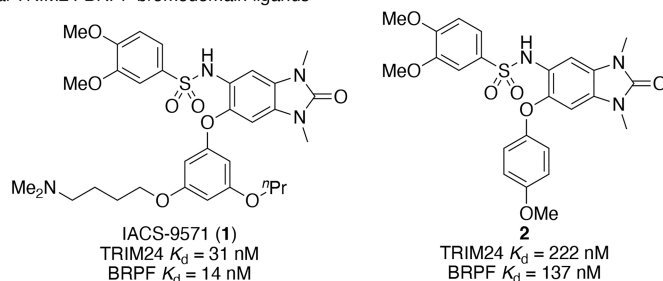


Figure 6. Occupancy of direct hydrophilic interactions (hydrogen bonds/salt bridges) between (A) H3K18Ac or (B) H3R17 and the TRIM BRDs during MD simulations (peptide carbon = yellow, protein carbon = white). Data are taken from 5×100 ns MD simulations (see SI for details on how these interactions were detected). The images of the proteins were made using the PyMOL Molecular Graphics System, version 2.5, Schrödinger, LLC.

A. Dual TRIM24 BRPF bromodomain ligands



B. Ligands reported as TRIM33 bromodomain ligands that cause AlphaScreen assay interference

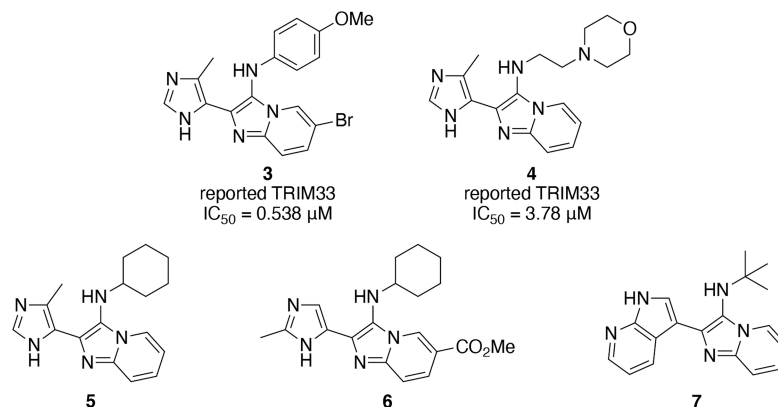


Figure 7. Previously reported ligands for the TRIM24 and TRIM33 BRDs. (A) TRIM24 ligand IACS-9571 (**1**) reported by Palmer et al.^{46,47} and compound **2** reported by Bennett et al.⁴⁸ with their literature K_d (ITC) values shown. (B) Selection of compounds reported by Qi and Pei,⁴⁹ which have also been synthesized in this study, with their literature IC_{50} (AlphaScreen) values shown. Our data show that all five compounds interfere with our TRIM24 and TRIM33 AlphaScreen assays. We could not detect binding of compounds **3** or **4** to the TRIM33 β BRD using either ITC or waterLOGSY.

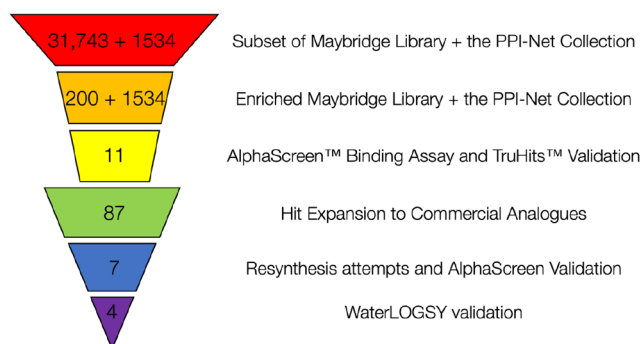


Figure 8. Screening and validation workflow used to identify ligands that bind the reader domains of TRIM24 and TRIM33 α . The workflow resulted in ligands 8–11 (Figure 9).

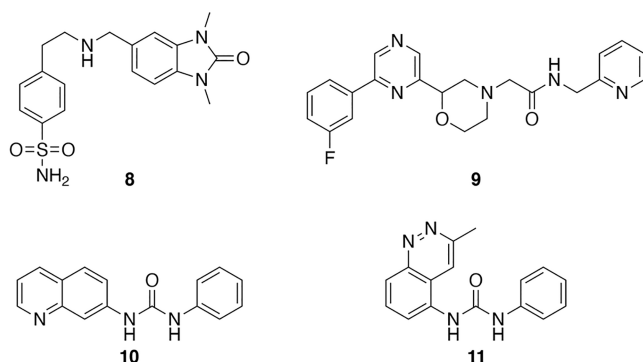


Figure 9. Compounds identified in the virtual screen and subsequently validated as ligands for TRIM24 and TRIM33.

TRIM24 PHD-BRD shows similar affinity for H3_{1–27}K9Me₃ ($K_d = 3.90 \pm 0.423 \mu\text{M}$) and H3_{1–27}K18Ac ($K_d = 4.37 \pm 0.430 \mu\text{M}$). The affinity of the two marks is additive, with H3_{1–27}K9Me₃K18Ac having higher affinity ($K_d = 1.94 \pm 0.111 \mu\text{M}$). This observation is in line with work from Ruthenburg et al., who showed that binding of H3K4Me₃ and H4K16Ac (in *trans*) is cooperative.⁵⁴ The TRIM33 α and

TRIM33 β PHD-BRD cassettes show very similar affinity for H3_{1–27}K9Me₃ ($K_d = 11.2 \pm 0.760 \mu\text{M}$ and $9.81 \pm 2.33 \mu\text{M}$, respectively) and H3_{1–27}K18Ac ($K_d = 10.0 \pm 0.319 \mu\text{M}$ and $8.95 \pm 0.643 \mu\text{M}$, respectively). Interestingly the affinity of these two marks is not additive for TRIM33 α as the dual modified H3_{1–27}K9Me₃K18Ac peptide shows a similar K_d value to the singly modified peptides ($K_d = 9.28 \pm 0.214 \mu\text{M}$). The dual modified H3_{1–27}K9Me₃K18Ac peptide has approximately double the affinity for the TRIM33 β PHD-BRD ($K_d = 4.78 \pm 0.200 \mu\text{M}$), compared to the singly modified peptides. The ITC N values from TRIM24 and TRIM33 range from 0.868 to 0.939 for the dual modified H3_{1–27}K9Me₃K18Ac peptide, indicating that the dual marked peptide is binding in *cis* under these conditions (Table S18). We note that these absolute K_d values observed using ITC are weaker than the IC₅₀ values observed using AlphaScreen, which we attribute to the competitive nature and inherent variability in the AlphaScreen format,⁵⁰ although the rank order of affinities is meaningful. The values observed using ITC are in line with those seen for other BRD–histone peptide interactions.¹⁵

Mutation Studies Identify the Contribution of Key Residues for H3 Binding. Having established the H3_{1–27}K9Me₃, H3_{1–27}K18Ac, and H3_{1–27}K9Me₃K18Ac peptides as binding partners for the TRIM33 α and TRIM33 β PHD-BRD, we next sought to investigate the contributions of key residues in the PHD and BRD to peptide recognition. To achieve this, we used the signal response curves for mutants of the TRIM24, TRIM33 α , and TRIM33 β PHD-BRD, and biotinylated peptides in the AlphaScreen assay. To probe binding to the PHD, we made the W828A mutation in TRIM24, and the W889A mutation in TRIM33 α and β . To probe BRD binding, we made both the N980A and N980F mutants in TRIM24 and the N1039F mutation in TRIM33 α and β . The N to F mutation has previously been shown to be more effective at preventing KAc binding to the BRD than the N to A mutation at the same position.⁵⁵

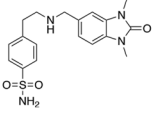
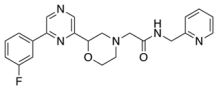
The W828A and W889A mutants generated no signal in the AlphaScreen assay when the proteins were incubated with varying concentrations of the H3_{1–27}K9Me₃ peptide. This

Table 4. Qualitative WaterLOGSY Binding of WT and Mutant TRIM Proteins^a

Compound	TRIM24			TRIM33 α			TRIM33 β		
	WT	N980F	W828A	WT	N1039F	W889A	WT	N1039F	W889A
8	✓	×	✓	✓	✓	✓	✓	?	✓
9	×	×	×	✓	✓	✓	✓	×	×
10	✓	✓	✓	✓	✓	✓	✓	✓	✓
11	✓	✓	✓	✓	✓	✓	✓	✓	✓

^a✓ is assigned to compounds that showed binding; ? is assigned when the result was ambiguous, and × is assigned when no-binding was observed.

Table 5. AlphaScreen Data for Compounds 8 and 9^a

Compound	Peptide in Assay	TRIM24 IC ₅₀ (μM)	TRIM33α IC ₅₀ (μM)	TRIM33β IC ₅₀ (μM)
8 	H3 ₁₋₂₇ K18Ac	102.6 ± 1.23	2.79 ± 0.83	18.4 ± 2.06
	H3 ₁₋₂₇ K9Me ₃	>250	>250	>250
	H3 ₁₋₂₇ K9Me ₃ K18Ac	>250	14.1 ± 1.62	126.2 ± 2.23
9 	H3 ₁₋₂₇ K18Ac	41.7 ± 7.82	51.8 ± 3.87	59.4 ± 5.73
	H3 ₁₋₂₇ K9Me ₃	41.8 ± 5.11	43.2 ± 5.67	78.6 ± 9.72
	H3 ₁₋₂₇ K9Me ₃ K18Ac	62.2 ± 4.15	56.5 ± 10.3	111.0 ± 13.5

^aNote that the IC₅₀ values cannot be compared between proteins. Errors are reported as the standard error of the mean between three measurements. A heatmap display is used with “hot” colors corresponding to lower IC₅₀ values.

indicates that this mutation abolishes PHD-mediated recognition of KMe₃ for all three proteins (Table 3). This result confirms the importance of W828/W889 in the recognition of the H3K9Me₃ modification. The affinity of the dual modified H3₁₋₂₇K9Me₃K18Ac was also reduced by the W828A/W889A mutations, compared to the wild-type proteins. The largest reduction in signal response for the H3₁₋₂₇K9Me₃K18Ac peptide occurred for the TRIM33α PHD-BRD, suggesting that the K9Me₃ modification provides a substantial contribution to the TRIM33α PHD-BRD affinity for the peptide, in line with the ITC data.

As expected, the N980F mutant was more effective than N980A at reducing binding of the H3₁₋₂₇K18Ac and H3₁₋₂₇K9Me₃K18Ac peptides to the TRIM24 PHD-BRD (Table 3). The N1039F mutation also reduced binding of the H3₁₋₂₇K18Ac peptide to the TRIM33β PHD-BRD, which has the canonical BRD. However, this mutation had no effect on the binding of the H3₁₋₂₇K18Ac and H3₁₋₂₇K9Me₃K18Ac peptides to the TRIM33α PHD-BRD. This result is consistent with the structural data showing that N1039 is located outside of the KAc binding pocket of the BRD. This result is particularly interesting when considered together with the previous AlphaScreen and ITC data (Tables 1 and 2). The ability of the TRIM33α PHD-BRD to bind to the H3₁₋₂₇K18Ac peptide and the fact that this binding is not disrupted by the N1039F mutation indicate that the K18Ac residue does bind in the BRD and that N1039 does not move into the KAc binding pocket to interact with K18Ac. This suggests that K18Ac forms interactions with the TRIM33α BRD that do not involve N1039.

Molecular Dynamics Simulations of the H3 Peptide Identify Recognition Patterns for H3K18Ac to TRIM24 and the TRIM33 Isoforms. To probe interaction of the H3 mimicking peptides with TRIM24, TRIM33α, and TRIM33β, we conducted molecular dynamics (MD) simulations. Using the X-ray crystal structure of the TRIM33α PHD-BRD bound to H3₁₋₂₀K9Me₃K14AcK18Ac (PDB code 3U5O),³⁶ models of each TRIM reader domain bound to H3₁₋₂₀K9Me₃K18Ac

were generated through alignment and used to perform MD simulations (see SI for details).

The simulations were analyzed using Protein–Ligand Interaction Profiler (PLIP)⁵⁶ to identify hydrophilic and hydrophobic contacts between the TRIM PHD-BRDs and the H3₁₋₂₀K9Me₃K18Ac peptide. Hydrophilic contacts were defined as hydrogen bonds, salt bridges, and cation– π interactions, while hydrophobic contacts were defined as interactions between close apolar peptide/protein atoms and π -stacking interactions (Figure 5). H3K18Ac made the most contacts with each BRD, consistent with the recognition of this modified residue by BRDs, but the nature of the interaction differed between systems. A similar number of hydrophilic and hydrophobic contacts were identified between the peptide and the TRIM24 or TRIM33β BRDs. Conversely, hydrophobic contacts formed the majority of interactions between H3K18Ac and the TRIM33α BRD.

The hydrophilic contacts between the BRDs and H3K18Ac and the flanking H3R17 residue were examined in greater detail as these two residues were found to display the most hydrophilic contacts with the TRIM-BRDs (Figure 6). In TRIM24 and TRIM33β, H3K18Ac directly interacts with N980/N1039 via the KAc carbonyl group (Figure 6A, Interaction 1), as has been observed for other canonical BRDs. This observation is consistent with experimental data showing that TRIM24 N980F and TRIM33β N1039F mutants have substantially disrupted binding to the H3₁₋₂₇K18Ac peptide (Table 3). In contrast, no direct interactions between H3K18Ac and N1039 in TRIM33α were observed, as this residue remains oriented away from the BRD pocket during simulations (consistent with the orientation shown in Figure 4A). We also examined other hydrogen bond interactions between H3K18Ac and Y935/Y993, but they were only observed intermittently (Figure 6A, Interaction 2). This analysis is also consistent with the TRIM33α crystallographic data (e.g., PDB code 3U5O) indicating that selective binding of both TRIM33 isoforms to H3K18Ac over other KAc residues is guided by an electrostatic interaction between E981 and H3R17 (Figure 6B, Interaction 1).³⁶ In addition to the

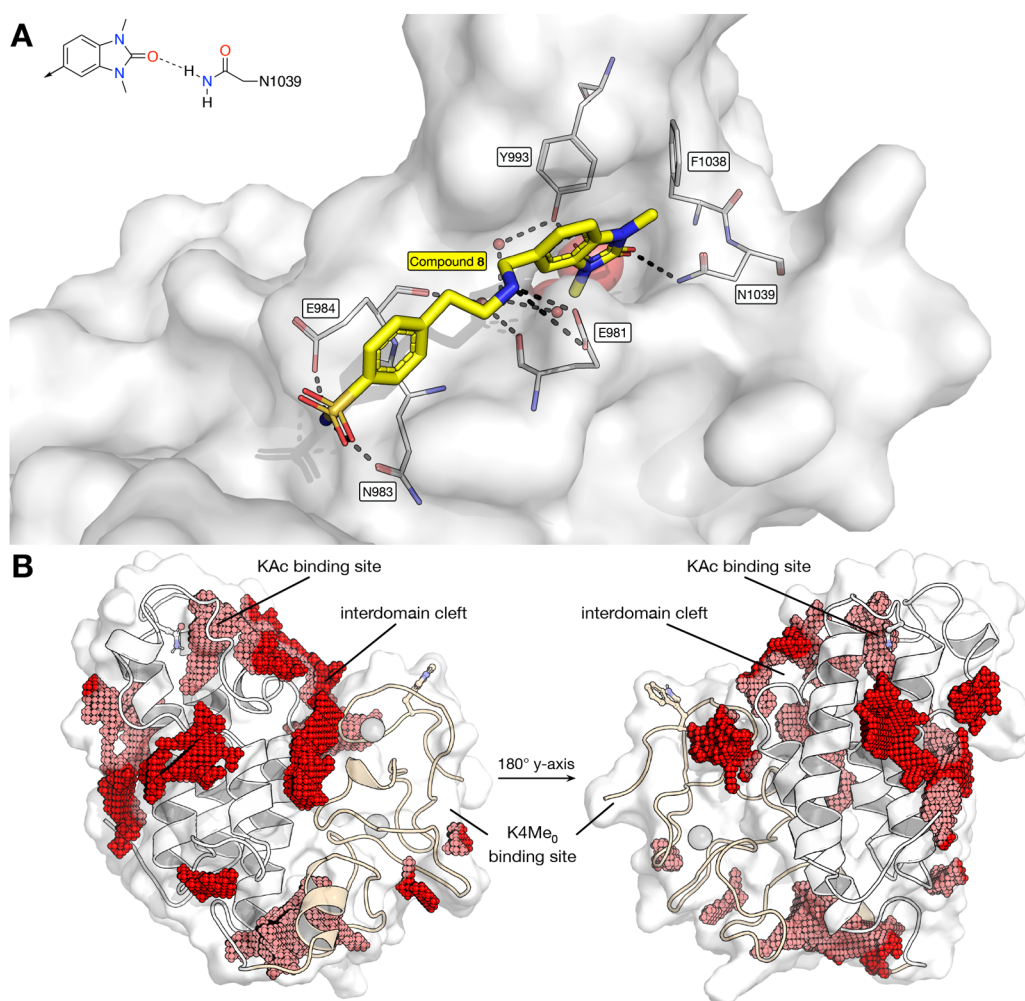


Figure 10. (A) Representation of compound **8** docked to the TRIM33 β BRD using MOE. The docking studies suggest that the benzoimidazolone moiety of compound **8** acts as the KAc mimic and that the compound binds to the TRIM33 β BRD by interacting with E981 and N1039. (B) Computational identification of cavities in the TRIM33 β reader cassette. A knowledge-based cavity detection was performed using CCDC's SuperStar package. This identified a deep cavity in the BRD, a long trench along the interdomain cleft, and a small region at the H3K4Me₀ binding site, among others. There was no binding site detected in the vicinity of the H3K9Me₃ binding region, consistent with its solvent-exposed nature. Figures generated using the PyMOL Molecular Graphics System, version 2.5, Schrödinger, LLC.

H3R17–E981 interaction, a less common interaction between H3R17 and a glutamate residue on the BC loop of TRIM24 and TRIM33 β was also observed (Figure 6B, Interaction 2). This might account for TRIM24 also showing affinity for H3K18Ac despite having A923 in place of E981 on the ZA loop.³⁶

Having observed minimal direct hydrogen bonding between the H3K18Ac side chain and Y993/N1039 in the TRIM33 α BRD, we also analyzed the possibility of water-mediated interactions in the BRD pocket (details in the SI). This analysis indicates that there is lower water density predicted in the KAc binding pocket of TRIM33 α compared to TRIM33 β or TRIM24 (Figure S11). This lower density might result from N1039 not being present to interact with the water molecules. The lower water density could impact the water-mediated hydrogen bonding between Y993 and the H3K18Ac side chain that is observed in other BRDs.⁵⁷ We then explored the hydrophobic contacts from the PLIP analysis to identify hydrophobic residues interacting with H3K18Ac, as TRIM33 α formed a substantially greater number of hydrophobic contacts

with H3K18Ac than the other BRDs (details in the SI). In this analysis, H3K18Ac was found to make more hydrophobic contacts with F1038 in TRIM33 α than F979/F1038 in TRIM24/TRIM33 β . This residue directly precedes N1039, and we hypothesize that in TRIM33 α this residue can fluctuate to form hydrophobic interactions with H3K18Ac and stabilize the H3K18Ac–BRD interaction (see SI for details). Taken together, the MD simulations suggest that TRIM33 α recognizes H3K18Ac mainly through hydrophobic contacts, while TRIM24 and TRIM33 β form a more balanced split of hydrophobic and hydrophilic interactions with H3K18Ac.

AlphaScreen Assay Established and Validated for Identifying TRIM24 and TRIM33 Ligands. Only two high affinity probes have been reported for the TRIM24 BRD, and both compounds also bind to the BRPF1 BRD (Figure 7A).^{46–48} A patent from Qi and Pei claims a series of TRIM33 BRD ligands identified using an AlphaScreen (Figure 7B).⁴⁹ The isoform of TRIM33 used in this work is not specified in the patent but was later confirmed to be TRIM33 α (Qi, personal communication). We investigated using the pre-

viously reported TRIM24 and TRIM33 ligands to help validate our assay. Our AlphaScreen assay results for the TRIM24 ligand 2 agree with the literature reports (Figure S2), as displacement of H3₁₋₂₇K18Ac was observed for TRIM24 but not for either isoform of TRIM33. An IC₅₀ value of 219 nM was obtained for compound 2 binding to the TRIM24 BRD-PHD, which is very similar to the K_d value of 222 nM reported by Bennett et al.⁴⁸ Three of the reported TRIM33 ligands (3, 4, and 6) showed apparent displacement of all three peptides from all three proteins in the AlphaScreen assay, with the additional two showing binding to TRIM24 and either weak or no binding to TRIM33 (Table S20, compounds 3–7).

To determine whether compounds 3–7 are genuine ligands for TRIM33, we employed an AlphaScreen TruHits screen.⁵⁸ The TruHits screen includes streptavidin-coated donor beads and biotinylated acceptor beads, which interact to generate a signal. Compounds that interfere with this control signal, such as fluorescence quenchers, insoluble light scatterers, ¹O₂ quenchers, and biotin mimetics, can be identified using this approach. In the TruHits screen,⁵⁹ significant assay interference was observed from all five compounds (3–7, Table S21), meaning that AlphaScreen data generated for these compounds are unreliable. We therefore sought to investigate TRIM33 binding of compounds 3 and 4 using ITC and waterLOGSY approaches (Figures S3–6). These compounds were selected as they have a range of reported IC₅₀ values for TRIM33. Neither compound showed binding to TRIM33β when assessed by ITC (Figures S3 and S4), using conditions based on the reported IC₅₀ values. To determine whether these compounds are weak binders to TRIM33β, we subjected them to a waterLOGSY assay against TRIM33β. Again, neither compound showed any binding to this protein (Figures S5 and S6). Based on these data, we have concluded that these compounds, at least in our hands, are interfering with the TRIM24 and TRIM33 AlphaScreen assay and do not bind to TRIM33β. However, the use of different protein isoforms may account for some of the observed discrepancies.

An Enriched High Throughput Screen Identified Ligands of the TRIM24 and TRIM33 Reader Domains. Having validated the AlphaScreen assay, we next sought to identify new ligands for TRIM33. For simplicity, we used the same peptides as the competing ligand in the AlphaScreen assay for TRIM24, TRIM33α, and TRIM33β. As these peptides have different affinity for each protein, IC₅₀ values generated are not comparable between proteins.

To select compounds to be used in the AlphaScreen assay, 31743 compounds from the Maybridge fragment library (Fisher Scientific), along with 1534 compounds from the PPI-Net collection, were screened *in silico* against TRIM24 and TRIM33α. Based on the results from this screen, we identified an enriched fragment library of 200 compounds selected for predicted affinity, reliability of binding mode, and synthetic tractability. These compounds, along with the entire PPI-Net library, were screened against TRIM24, TRIM33α, and TRIM33β using a qualitative AlphaScreen response assay (data not shown). In this assay, the compounds were tested at two concentrations, 30 μM and 150 μM, as a rapid method of establishing activity. This study identified seven molecules from the PPI-Net library and four molecules from the Maybridge library as potential binders to one or more of the TRIM24 and TRIM33 reader domains. To increase the number of putative ligands, we identified additional ligands in the Maybridge Fragment library that show similarity to the

hits, based on the Tanimoto coefficient (Figure 8).⁵⁹ We only selected ligands that have a solubility forecast index (SFI)⁶⁰ of <6.5. After validation of these molecules using NMR WaterLOGSY experiments and AlphaScreen TruHits screens (data not shown), four promising lead compounds, 8–11, were identified (Figure 9).

Compound 8 contains the dimethylbenzimidazolone motif, which acts as the KAc mimic in the TRIM24 BRD ligands 1 and 2, suggesting that this compound could bind to the TRIM33 BRD. Compounds 9–11, however, possess no commonly employed KAc mimics, making it harder to predict their site of binding. To investigate where these compounds bind on the TRIM24 or 33 PHD-BRD cassette, we performed waterLOGSY experiments using the wild-type and mutant reader domains (Table 4). As expected, compound 8 bound to the WT BRDs of TRIM24, TRIM33α, and TRIM33β. It showed no binding to the TRIM24 N980F mutant and no clear binding to the TRIM33β N1039F mutant, as would be expected for a compound binding to the BRD. The binding of this compound was unaffected by the W889A or W828A mutants, indicating that it does not bind to the PHD of either TRIM24 or TRIM33. Compound 9 showed no binding to TRIM24, but it does bind to the WT TRIM33α and TRIM33β. Binding to TRIM33β, but not TRIM33α, was disrupted by both the W889A and N1039F mutations, suggesting that this compound interacts with both the BRD and PHD or binds between these domains. Compounds 10 and 11 bind to all three proteins, and their binding was unaffected by any of the mutants, indicating that these compounds do not bind to the BRD or PHD.

Dose response AlphaScreen assays were performed to determine IC₅₀ values of fragments 8 and 9 for each TRIM protein domain (Table 5). Three peptides were used in this assay, H3₁₋₂₇K18Ac that detects binding to the BRD, H3₁₋₂₇K9Me₃ that detects binding to the PHD, and H3₁₋₂₇K9Me₃K18Ac that detects binding to both domains. As these peptides have different binding affinities to the BRDs and PHDs, IC₅₀ values obtained using two different peptides cannot be compared. Using the H3₁₋₂₇K18Ac peptide, compound 8 showed low affinity for TRIM24 BRD but IC₅₀ values of 2.79 ± 0.83 μM and 18.4 ± 2.06 μM for TRIM33α and TRIM33β, respectively. This compound showed no affinity for the TRIM24 or TRIM33 PHDs when using the H3₁₋₂₇K9Me₃ peptide, consistent with the hypothesis that this compound binds to the BRD. Compound 8 also showed only very weak binding to BRD4(1), a representative member of the BET family of BCPs, at concentrations of >100 μM when assessed using an AlphaScreen assay (Figure S8).^{50,51,62}

Given its similarity to previously reported TRIM24 BRD ligands,^{46–48} we proposed that compound 8 might occupy the KAc binding pocket of the TRIM33 BRD. Preliminary docking studies, using MOE, suggest that compound 8 (Figure 10A) can reside in the KAc binding pocket of TRIM33. The benzimidazolone is predicted to act as the KAc mimic, with the oxygen atom proposed to form hydrogen bonds with N1039 and, via a structured water molecule, Y993. The benzylic amine is predicted to form a salt bridge with E981, which is the residue that binds to H3R17 contributing to the recognition of the H3 peptide (see above). This interaction is likely important for ligand affinity and explains the selectivity of this compound for TRIM33 over TRIM24, as the equivalent residue in TRIM24 is an alanine (A923). While reasonable,

further computational studies are required to improve our understanding of the proposed binding mode of compound 8.

Compound 9 shows weak affinity to both TRIM24 and TRIM33 when any of the peptides were used, consistent with the idea that this compound does not bind to exclusively the BRD or PHD of these proteins. To identify possible binding locations for compounds 9–11, beyond the BRD and KAc, the CCDC SuperStar package was used to detect cavities in TRIM33 β . This approach identified the KAc binding site, a shallow site at the K4Me₀ binding region, and a larger cavity between the BRD and PHD (Figure 10B). The analysis also showed there was a cavity at the base of the construct. Based on these results, it is possible that compound 9 binds in this interdomain cleft, explaining the AlphaScreen assay results.

The low number of hits from our screen, with only 4 compounds confirmed from a total of 1821 screened (0.22% hit rate), coupled with the low affinity of these hits, indicates that TRIM33 is not an easily ligandable target based on the criteria of Vukovic and Huggins.⁶¹ This finding is consistent with the work of Vidler et al.⁶² who analyzed the druggability of a range of bromodomains, and classified the TRIM24 and TRIM33 difficult to drug. Given the challenges associated with identifying ligands for TRIM33, our data indicate that compound 8 is an important hit that could form the basis of selective, high affinity ligands for the TRIM33 BRDs.

CONCLUSIONS

In conclusion, we report a comprehensive investigation into both peptide and small molecule ligands for the TRIM33 BRDs and PHDs. We have shown that, while the structure of the TRIM33 α and TRIM33 β BRDs differ in terms of N1039 location, they can both still bind to H3K18Ac with similar affinity. Interestingly, computational studies suggest that this affinity is derived mainly from hydrophobic interactions in the case of TRIM33 α but from a mixture of hydrophilic and hydrophobic contacts for TRIM33 β . This observation has implications for future ligand design. An AlphaScreen assay for the TRIM33 PHD-BRDs had low hit rate of 0.22%, indicating that TRIM33 PHDs and BRDs are difficult targets to ligand. However, we did identify compound 8, which possesses a known KAc mimic; waterLOGSY experiments and initial docking studies predict that this compound binds to the TRIM33 BRDs. Furthermore, this compound shows little or no affinity for the BRDs of TRIM24 and BRD4(1). Given the difficulty of identifying ligands for TRIM33, compound 8 is an important hit that will enable development of selective high affinity ligands for the TRIM33 BRDs. The role of TRIM33 in the DNA damage response means that these compounds are of therapeutic interest for oncology indications. In addition, TRIM33 possesses E3 ligase activity, and so the identification of ligands for its BRDs raises the possibility that PROTACs that recruit TRIM33 to degrade a protein of interest can be developed. It remains to be seen whether ligands that are selective for TRIM33 α or TRIM33 β can be developed and whether they have different biological activity, either individually or as E3 ligase ligands in PROTACs. The data that we report here provide a strong foundation for such investigations into these important proteins.

ASSOCIATED CONTENT

Supporting Information

The Supporting Information is available free of charge at <https://pubs.acs.org/doi/10.1021/acschembio.2c00266>.

Biological methods, chemical experimental section, computational methods sections, supplementary figures, and tables, NMR spectra and HPLC traces for compound 8 (PDF)

The preliminary PDB validation report for PDB entry 7ZDD (PDF)

Accession Codes

The atomic coordinates and structure factors of human TRIM33 BRD-PHD isoform B in complex with the H3K9Ac peptide has been deposited in the Protein Data Bank (wwPDB) with accession code 5MR8. The atomic coordinates and structure factors of human TRIM33 BRD-PHD isoform B in complex with the H3K10Ac peptide has been deposited in the Protein Data Bank (wwPDB) with accession code 7ZDD.

AUTHOR INFORMATION

Corresponding Author

Stuart J. Conway – Department of Chemistry, Chemistry Research Laboratory, University of Oxford, Oxford OX1 3TA, U.K.; orcid.org/0000-0002-5148-117X; Email: stuart.conway@chem.ox.ac.uk

Authors

Angelina R. Sekirnik – Department of Chemistry, Chemistry Research Laboratory, University of Oxford, Oxford OX1 3TA, U.K.

Jessica K. Reynolds – Department of Chemistry, Chemistry Research Laboratory, University of Oxford, Oxford OX1 3TA, U.K.

Larissa See – Department of Chemistry, Chemistry Research Laboratory, University of Oxford, Oxford OX1 3TA, U.K.

Joseph P. Bluck – Department of Chemistry, Chemistry Research Laboratory, University of Oxford, Oxford OX1 3TA, U.K.; Department of Biochemistry, University of Oxford, Oxford OX1 3QU, U.K.; Present Address: Computational Molecular Design, Pharmaceuticals, R&D, Bayer AG, 13342 Berlin, Germany

Amy R. Scorah – Department of Chemistry, Chemistry Research Laboratory, University of Oxford, Oxford OX1 3TA, U.K.

Cynthia Tallant – Nuffield Department of Clinical Medicine, Structural Genomics Consortium, University of Oxford, Oxford OX3 3TA, U.K.

Bernadette Lee – Department of Chemistry, Chemistry Research Laboratory, University of Oxford, Oxford OX1 3TA, U.K.

Katarzyna B. Leszczynska – Oxford Institute for Radiation Oncology, University of Oxford, Oxford OX3 7DQ, U.K.; Present Address: Laboratory of Molecular Neurobiology, Neurobiology Center, Nencki Institute of Experimental Biology, Polish Academy of Sciences, Warsaw, Poland.

Rachel L. Grimley – Worldwide Medicinal Chemistry, Discovery Biology, Pfizer Ltd, Cambridge CB21 6GS, U.K.

R. Ian Storer – Worldwide Medicinal Chemistry, Discovery Biology, Pfizer Ltd, Cambridge CB21 6GS, U.K.

Marta Malattia – Evotec (UK) Ltd, Oxfordshire OX14 4RZ, U.K.

Sara Crespillo – Evotec (UK) Ltd, Oxfordshire OX14 4RZ, U.K.

Sofia Caria – Evotec (UK) Ltd, Oxfordshire OX14 4RZ, U.K.

Stephanie Duclos – Evotec (UK) Ltd, Oxfordshire OX14 4RZ, U.K.

Ester M. Hammond – Oxford Institute for Radiation Oncology, University of Oxford, Oxford OX3 7DQ, U.K.; orcid.org/0000-0002-2335-3146

Stefan Knapp – Institute of Pharmaceutical Chemistry, Goethe University, D-60438 Frankfurt am Main, Germany; Structural Genomics Consortium, Buchmann Institute for Life Sciences (BMLS), Goethe University, D-60438 Frankfurt am Main, Germany; orcid.org/0000-0001-5995-6494

Garrett M. Morris – Department of Statistics, University of Oxford, Oxford OX1 3LB, U.K.

Fernanda Duarte – Department of Chemistry, Chemistry Research Laboratory, University of Oxford, Oxford OX1 3TA, U.K.; orcid.org/0000-0002-6062-8209

Philip C. Biggin – Department of Biochemistry, University of Oxford, Oxford OX1 3QU, U.K.; orcid.org/0000-0001-5100-8836

Complete contact information is available at:

<https://pubs.acs.org/10.1021/acscchembio.2c00266>

Author Contributions

[‡]A. R. Sekirnik and J.K.R. contributed equally. The manuscript was written through contributions of all authors. All authors have given approval to the final version of the manuscript.

Notes

The authors declare no competing financial interest.

ACKNOWLEDGMENTS

A. R. Sekirnik thanks Pfizer Neusentis and the EPSRC for studentship support. J.K.R. and A. R. Scorch thank the EPSRC Centre for Doctoral Training in Synthesis for Biology and Medicine (EP/L015838/1) and the EPSRC (EP/S03658X/1) for support. J.P.B. thanks the EPSRC and GlaxoSmithKline for studentship support via the Systems Approaches to Biomedical Sciences Centre for Doctoral Training (EP/G037280/1). B.L. is grateful to the Agency for Science, Technology and Research (A*STAR) and the Centre for Doctoral Training in Synthesis for Biology and Medicine for a studentship, generously supported by GlaxoSmithKline, MSD, Syngenta, and Vertex. This project made use of time on JADE2 granted via the UK High-End Computing Consortium for Biomolecular Simulation, HECBioSim (<https://www.hecbiosim.ac.uk/>), supported by EPSRC (EP/T022205/1). We are grateful to J. Massagué for provision of plasmids and O. Fedorov (SGC) for provision of the TRIM24 control compound. P.C.B. thanks Lady Margaret Hall, Oxford, for research funding. S.J.C. and E.M.H. thank Oxford University Innovation for the award of a Lab282 grant (OUI17491). S.J.C. thanks St Hugh's College, Oxford, for research funding.

ABBREVIATIONS

TRIM, tripartite motif containing protein; BRD, bromodomain; PHD, plant homeodomain; KAc, acetylated lysine; KMe_n, methylated lysine

REFERENCES

- (1) Hatakeyama, S. TRIM Family Proteins: Roles in Autophagy, Immunity, and Carcinogenesis. *Trends Biochem. Sci.* **2017**, *42*, 297–311.
- (2) D'Amico, F.; Mukhopadhyay, R.; Ovaa, H.; Mulder, M. P. C. Targeting TRIM Proteins: A Quest towards Drugging an Emerging Protein Class. *ChemBioChem.* **2021**, *22*, 2011–2031.
- (3) Amato, A.; Lucas, X.; Bortoluzzi, A.; Wright, D.; Ciulli, A. Targeting Ligandable Pockets on Plant Homeodomain (PHD) Zinc

Finger Domains by a Fragment-Based Approach. *ACS Chem. Biol.* **2018**, *13*, 915–921.

(4) Laity, J. H.; Lee, B. M.; Wright, P. E. Zinc Finger Proteins: New Insights into Structural and Functional Diversity. *Curr. Opin. Struct. Biol.* **2001**, *11*, 39–46.

(5) Slama, P.; Geman, D. Identification of Family-Determining Residues in PHD Fingers. *Nucleic Acids Res.* **2011**, *39*, 1666–1679.

(6) Arrowsmith, C. H.; Schapira, M. Targeting Non-Bromodomain Chromatin Readers. *Nat. Struct. Mol. Biol.* **2019**, *26*, 863–869.

(7) Sbardella, G. Methyl-Readers and Inhibitors. *Topics in Medicinal Chemistry*; Springer, 2019; Vol. 33, pp 339–399. DOI: [10.1007/7355_2019_78](https://doi.org/10.1007/7355_2019_78).

(8) Spiliotopoulos, D.; Spitaleri, A.; Musco, G. Exploring PHD Fingers and H3K4Me0 Interactions with Molecular Dynamics Simulations and Binding Free Energy Calculations: AIRE-PHD1, a Comparative Study. *PLoS One* **2012**, *7*, e46902.

(9) Sanchez, R.; Zhou, M.-M. The PHD Finger: A Versatile Epigenome Reader. *Trends Biochem. Sci.* **2011**, *36*, 364–372.

(10) Baker, L. A.; Allis, C. D.; Wang, G. G. PHD Fingers in Human Diseases: Disorders Arising from Misinterpreting Epigenetic Marks. *Mutation Research - Fundamental and Molecular Mechanisms of Mutagenesis* **2008**, *647*, 3–12.

(11) Ferri, E.; Petosa, C.; McKenna, C. E. Bromodomains: Structure, Function and Pharmacology of Inhibition. *Biochem. Pharmacol.* **2016**, *106*, 1–18.

(12) Cochran, A. G.; Conery, A. R.; Sims, R. J. Bromodomains: A New Target Class for Drug Development. *Nat. Rev. Drug Disc.* **2019**, *18*, 609–628.

(13) Schiedel, M.; Moroglu, M.; Ascough, D. M. H.; Chamberlain, A. E. R.; Kamps, J. J. A. G.; Sekirnik, A. R.; Conway, S. J. Chemical Epigenetics: The Impact of Chemical and Chemical Biology Techniques on Bromodomain Target Validation. *Angew. Chem., Int. Ed.* **2019**, *58*, 17930–17952.

(14) Conway, S. J. Bromodomains: Are Readers Right for Epigenetic Therapy? *ACS Med. Chem. Lett.* **2012**, *3*, 691–694.

(15) Filippakopoulos, P.; Picaud, S.; Mangos, M.; Keates, T.; Lambert, J.-P.; Barsyte-Lovejoy, D.; Felletar, I.; Volkmer, R.; Müller, S.; Pawson, T.; et al. Histone Recognition and Large-Scale Structural Analysis of the Human Bromodomain Family. *Cell* **2012**, *149*, 214–231.

(16) Dhalluin, C.; Carlson, J. E.; Zeng, L.; He, C.; Aggarwal, A. K.; Zhou, M.-M.; Zhou, M.-M. Structure and Ligand of a Histone Acetyltransferase Bromodomain. *Nature* **1999**, *399*, 491–496.

(17) Zeng, L.; Zhou, M. M. Bromodomain: An Acetyl-Lysine Binding Domain. *FEBS Lett.* **2002**, *513*, 124–128.

(18) Hewings, D. S.; Rooney, T. P. C.; Jennings, L. E.; Hay, D. A.; Schofield, C. J.; Brennan, P. E.; Knapp, S.; Conway, S. J. Progress in the Development and Application of Small Molecule Inhibitors of Bromodomain–Acetyl-Lysine Interactions. *J. Med. Chem.* **2012**, *55*, 9393–9413.

(19) Crawford, T. D.; Tsui, V.; Flynn, E. M.; Wang, S.; Taylor, A. M.; Côté, A.; Audia, J. E.; Beresini, M. H.; Burdick, D. J.; Cummings, R.; et al. Diving into the Water: Inducible Binding Conformations for BRD4, TAF1(2), BRD9, and CECR2 Bromodomains. *J. Med. Chem.* **2016**, *59*, 5391–5402.

(20) Aldeghi, M.; Ross, G. A.; Bodkin, M. J.; Essex, J. W.; Knapp, S.; Biggin, P. C. Large-Scale Analysis of Water Stability in Bromodomain Binding Pockets with Grand Canonical Monte Carlo. *Commun. Chem.* **2018**, *1*, 19.

(21) Sekirnik née Measures, A. R.; Hewings, D. S.; Theodoulou, N. H.; Jursins, L.; Lewendon, K. R.; Jennings, L. E.; Rooney, T. P. C.; Heightman, T. D.; Conway, S. J. Isoxazole-Derived Amino Acids Are Bromodomain-Binding Acetyl-Lysine Mimics: Incorporation into Histone H4 Peptides and Histone H3. *Angew. Chem., Int. Ed.* **2016**, *55*, 8353–8357.

(22) Kulkarni, A.; Oza, J.; Yao, M.; Sohail, H.; Ginja, V.; Tomas-Loba, A.; Horejsi, Z.; Tan, A. R.; Boulton, S. J.; Ganesan, S. Tripartite Motif-Containing 33 (TRIM33) Protein Functions in the Poly(ADP-Ribose) Polymerase (PARP)-Dependent DNA Damage Response

through Interaction with Amplified in Liver Cancer 1 (ALC1) Protein. *J. Biol. Chem.* **2013**, *288*, 32357–32369.

(23) Tsai, W. W.; Wang, Z.; Yiu, T. T.; Akdemir, K. C.; Xia, W.; Winter, S.; Tsai, C.-Y.; Shi, X.; Schwarzer, D.; Plunkett, W.; et al. TRIM24 Links a Non-Canonical Histone Signature to Breast Cancer. *Nature* **2010**, *468*, 927–932.

(24) Fang, Z.; Deng, J.; Zhang, L.; Xiang, X.; Yu, F.; Chen, J.; Feng, M.; Xiong, J. TRIM24 Promotes the Aggression of Gastric Cancer via the Wnt/ β -Catenin Signaling Pathway. *Oncology Lett.* **2017**, *13*, 1797–1806.

(25) Li, H.; Sun, L.; Tang, Z.; Fu, L.; Xu, Y.; Li, Z.; Luo, W.; Qiu, X.; Wang, E. Overexpression of TRIM24 Correlates with Tumor Progression in Non-Small Cell Lung Cancer. *PLoS One* **2012**, *7*, e37657.

(26) Gchijian, L. N.; Buckley, D. L.; Lawlor, M. A.; Reyes, J. M.; Paulk, J.; Ott, C. J.; Winter, G. E.; Erb, M. A.; Scott, T. G.; Xu, M.; et al. Functional TRIM24 Degrader via Conjugation of Ineffective Bromodomain and VHL Ligands. *Nat. Chem. Biol.* **2018**, *14*, 405–412.

(27) Groner, A. C.; Cato, L.; de Tribolet-Hardy, J.; Bernasocchi, T.; Janouskova, H.; Melchers, D.; Houtman, R.; Cato, A. C. B.; Tschopp, P.; Gu, L.; et al. TRIM24 Is an Oncogenic Transcriptional Activator in Prostate Cancer. *Cancer Cell* **2016**, *29*, 846–858.

(28) Liu, X.; Huang, Y.; Yang, D.; Li, X.; Liang, J.; Lin, L.; Zhang, M.; Zhong, K.; Liang, B.; Li, J. Overexpression of TRIM24 Is Associated with the Onset and Progress of Human Hepatocellular Carcinoma. *PLoS One* **2014**, *9*, e85462.

(29) Wang, J.; Zhu, J.; Dong, M.; Yu, H.; Dai, X.; Li, K. Knockdown of Tripartite Motif Containing 24 by Lentivirus Suppresses Cell Growth and Induces Apoptosis in Human Colorectal Cancer Cells. *Oncology Res.* **2014**, *22*, 39–45.

(30) Appikonda, S.; Thakkar, K. N.; Barton, M. C. Regulation of Gene Expression in Human Cancers by TRIM24. *Drug Disc. Today: Technologies* **2016**, *19*, 57–63.

(31) Xue, J.; Lin, X.; Chiu, W. T.; Chen, Y. H.; Yu, G.; Liu, M.; Feng, X. H.; Sawaya, R.; Medema, R. H.; Hung, M. C.; et al. Sustained Activation of SMAD3/SMAD4 by FOXM1 Promotes TGF- β -Dependent Cancer Metastasis. *J. Clinical Invest.* **2014**, *124*, 564–579.

(32) Wang, L.; Yang, H.; Lei, Z.; Zhao, J.; Chen, Y.; Chen, P.; Li, C.; Zeng, Y.; Liu, Z.; Liu, X.; et al. Repression of TIF1 γ by SOX2 Promotes TGF- β -Induced Epithelial-Mesenchymal Transition in Non-Small-Cell Lung Cancer. *Oncogene* **2016**, *35*, 867–877.

(33) Jingushi, K.; Ueda, Y.; Kita, K.; Hase, H.; Egawa, H.; Ohshio, I.; Kawakami, R.; Kashiwagi, Y.; Tsukada, Y.; Kobayashi, T.; et al. MiR-629 Targets TRIM33 to Promote TGF β /Smad Signaling and Metastatic Phenotypes in CcRCC. *Mol. Cancer Res.* **2015**, *13*, 565–574.

(34) Xue, J.; Chen, Y.; Wu, Y.; Wang, Z.; Zhou, A.; Zhang, S.; Lin, K.; Aldape, K.; Majumder, S.; Lu, Z.; et al. Tumour Suppressor TRIM33 Targets Nuclear β -Catenin Degradation. *Nat. Commun.* **2015**, *6*, 6156.

(35) Agricola, E.; Randall, R. A.; Gaarenstroom, T.; Dupont, S.; Hill, C. S. Recruitment of TIF1-Gamma to Chromatin via Its PHD Finger-Bromodomain Activates Its Ubiquitin Ligase and Transcriptional Repressor Activities. *Mol. Cell* **2011**, *43*, 85–96.

(36) Xi, Q.; Wang, Z.; Zaromytidou, A.-I.; Zhang, X. H.-F.; Chow-Tsang, L.-F.; Liu, J. X.; Kim, H.; Barlas, A.; Manova-Todorova, K.; Kaartinen, V.; et al. A Poised Chromatin Platform for TGF- β Access to Master Regulators. *Cell* **2011**, *147*, 1511–1524.

(37) Wang, E.; Kawaoka, S.; Roe, J.-S.; Shi, J.; Hohmann, A. F.; Xu, Y.; Bhagwat, A. S.; Suzuki, Y.; Kinney, J. B.; Vakoc, C. R. The Transcriptional Cofactor TRIM33 Prevents Apoptosis in B Lymphoblastic Leukemia by Deactivating a Single Enhancer. *Elife* **2015**, *4*, e06377.

(38) Yu, C.; Ding, Z.; Liang, H.; Zhang, B.; Chen, X. The Roles of TIF1 γ in Cancer. *Frontiers in Oncology* **2019**, *9*, 979.

(39) Chen, J.; Wang, Z.; Guo, X.; Li, F.; Wei, Q.; Chen, X.; Gong, D.; Xu, Y.; Chen, W.; Liu, Y.; et al. TRIM66 Reads Unmodified

H3R2K4 and H3K56ac to Respond to DNA Damage in Embryonic Stem Cells. *Nat. Commun.* **2019**, *10*, 4273.

(40) Reymond, A.; Meroni, G.; Fantozi, A.; Merla, G.; Cairo, S.; Luzi, L.; Riganelli, D.; Zanaria, E.; Messali, S.; Cainarca, S.; et al. The Tripartite Motif Family Identifies Cell Compartments. *EMBO J.* **2001**, *20*, 2140–2151.

(41) Eberl, H. C.; Spruijt, C. G.; Kelstrup, C. D.; Vermeulen, M.; Mann, M. A Map of General and Specialized Chromatin Readers in Mouse Tissues Generated by Label-Free Interaction Proteomics. *Mol. Cell* **2013**, *49*, 368–378.

(42) Brand, M.; Measures, A. M.; Wilson, B. G.; Cortopassi, W. A.; Alexander, R.; Höss, M.; Hewings, D. S.; Rooney, T. P. C.; Paton, R. S.; Conway, S. J. Small Molecule Inhibitors of Bromodomain–Acetyl-Lysine Interactions. *ACS Chem. Biol.* **2015**, *10*, 22–39.

(43) Theodoulou, N. H.; Tomkinson, N. C. O.; Prinjha, R. K.; Humphreys, P. G. Clinical Progress and Pharmacology of Small Molecule Bromodomain Inhibitors. *Curr. Opin. Chem. Biol.* **2016**, *33*, 58–66.

(44) Theodoulou, N. H.; Tomkinson, N. C. O.; Prinjha, R. K.; Humphreys, P. G. Progress in the Development of Non-BET Bromodomain Chemical Probes. *ChemMedChem* **2016**, *11*, 477–487.

(45) Clegg, M. A.; Tomkinson, N. C. O.; Prinjha, R. K.; Humphreys, P. G. Advancements in the Development of Non-BET Bromodomain Chemical Probes. *ChemMedChem* **2019**, *14*, 362–385.

(46) Palmer, W. S.; Poncet-Montange, G.; Liu, G.; Petrocchi, A.; Reyna, N.; Subramanian, G.; Theroff, J.; Yau, A.; Kost-Alimova, M.; Bardenhagen, J. P.; et al. Structure-Guided Design of IACS-9571, a Selective High-Affinity Dual TRIM24-BRPF1 Bromodomain Inhibitor. *J. Med. Chem.* **2016**, *59*, 1440–1454.

(47) Palmer, W. S. Development of Small Molecule Inhibitors of BRPF1 and TRIM24 Bromodomains. *Drug Disc. Today: Technologies* **2016**, *19*, 65–71.

(48) Bennett, J.; Fedorov, O.; Tallant, C.; Monteiro, O.; Meier, J.; Gamble, V.; Savitsky, P.; Nunez-Alonso, G. A.; Haendler, B.; Rogers, C.; et al. Discovery of a Chemical Tool Inhibitor Targeting the Bromodomains of TRIM24 and BRPF. *J. Med. Chem.* **2016**, *59*, 1642–1647.

(49) Qi, J.; Pei, C. Inhibitors of TRIM33 and Methods of Use. U.S. PatentUS16/604030, 2020.

(50) Philpott, M.; Yang, J.; Tumber, T.; Fedorov, O.; Uttarkar, S.; Filippakopoulos, P.; Picaud, S.; Keates, T.; Felletar, I.; Ciulli, A.; et al. Bromodomain-Peptide Displacement Assays for Interactome Mapping and Inhibitor Discovery. *MolBioSyst.* **2011**, *7*, 2899–2908.

(51) Hewings, D. S.; Wang, M.; Philpott, M.; Fedorov, O.; Uttarkar, S.; Filippakopoulos, P.; Picaud, S.; Vuppasetty, C.; Marsden, B.; Knapp, S.; et al. 3,5-Dimethylisoxazoles Act As Acetyl-Lysine-Mimetic Bromodomain Ligands. *J. Med. Chem.* **2011**, *54*, 6761–6770.

(52) Ahel, D.; Horejsi, Z.; Wiechens, N.; Polo, S. E.; Garcia-Wilson, E.; Ahel, I.; Flynn, H.; Skehel, M.; West, S. C.; Jackson, S. P.; et al. Poly(ADP-Ribose)-Dependent Regulation of DNA Repair by the Chromatin Remodeling Enzyme ALC1. *Science* **2009**, *325*, 1240–1243.

(53) Tsai, W.-W.; Wang, Z.; Yiu, T. T.; Akdemir, K. C.; Xia, W.; Winter, S.; Tsai, C.-Y.; Shi, X.; Schwarzer, D.; Plunkett, W.; et al. TRIM24 Links a Non-Canonical Histone Signature to Breast Cancer. *Nature* **2010**, *468*, 927–932.

(54) Ruthenburg, A. J.; Li, H.; Milne, T. A.; Dewell, S.; McGinty, R. K.; Yuen, M.; Ueberheide, B.; Dou, Y.; Muir, T. W.; Patel, D. J.; et al. Recognition of a Mononucleosomal Histone Modification Pattern by BPTF via Multivalent Interactions. *Cell* **2011**, *145*, 692–706.

(55) Philpott, M.; Rogers, C. M.; Yapp, C.; Wells, C.; Lambert, J.-P.; Strain-Damerell, C.; Burgess-Brown, N. A.; Gingras, A.-C.; Knapp, S.; Müller, S. Assessing Cellular Efficacy of Bromodomain Inhibitors Using Fluorescence Recovery after Photobleaching. *Epigenetics & Chromatin* **2014**, *7*, 14.

(56) Salentin, S.; Schreiber, S.; Haupt, V. J.; Adasme, M. F.; Schroeder, M. PLIP: Fully Automated Protein–Ligand Interaction Profiler. *Nucleic Acids Res.* **2015**, *43*, W443–W447.

(57) Owen, D. J.; Ornaghi, P.; Yang, J. C.; Lowe, N.; Evans, P. R.; Ballario, P.; Neuhaus, D.; Filetici, P.; Travers, A. A. The Structural Basis for the Recognition of Acetylated Histone H4 by the Bromodomain of Histone Acetyltransferase Gcn5p. *EMBO J.* **2000**, *19*, 6141–6149.

(58) Yasgar, A.; Jadhav, A.; Simeonov, A.; Coussens, N. P. AlphaScreen-Based Assays: Ultra-High-Throughput Screening for Small-Molecule Inhibitors of Challenging Enzymes and Protein-Protein Interactions. In *High Throughput Screening*; Janzen, W., Ed.; Humana Press: New York, NY, 2016; Vol. 1439. DOI: [10.1007/978-1-4939-3673-1_5](https://doi.org/10.1007/978-1-4939-3673-1_5).

(59) Bero, S. A.; Muda, A. K.; Choo, Y. H.; Muda, N. A.; Pratama, S. F. Similarity Measure for Molecular Structure: A Brief Review. *Journal of Physics: Conference Series* **2017**, *892*, 012015.

(60) Hill, A. P.; Young, R. J. Getting Physical in Drug Discovery: A Contemporary Perspective on Solubility and Hydrophobicity. *Drug Disc. Today* **2010**, *15*, 648–655.

(61) Vukovic, S.; Huggins, D. J. Quantitative Metrics for Drug–Target Ligandability. *Drug Disc. Today* **2018**, *23*, 1258–1266.

(62) Vidler, L. R.; Brown, N.; Knapp, S.; Hoelder, S. Druggability Analysis and Structural Classification of Bromodomain Acetyl-Lysine Binding Sites. *J. Med. Chem.* **2012**, *55*, 7346–7359.

Recommended by ACS

Covalent-Fragment Screening of BRD4 Identifies a Ligandable Site Orthogonal to the Acetyl-Lysine Binding Sites

Michael D. Olp, Brian C. Smith, *et al.*

MARCH 09, 2020
ACS CHEMICAL BIOLOGY

[READ !\[\]\(b792654f2cef9719eabeb6c5be00811e_img.jpg\)](#)

Discovery and Mechanism of Small Molecule Inhibitors Selective for the Chromatin-Binding Domains of Oncogenic UHRF1

Wallace H. Liu, John M. Denu, *et al.*

FEBRUARY 10, 2022
BIOCHEMISTRY

[READ !\[\]\(84f47badaad7772cd95667a7c387a639_img.jpg\)](#)

Molecular Insights into the Recognition of Acetylated Histone Modifications by the BRPF2 Bromodomain

Soumen Barman, Babu Sudhamalla, *et al.*

AUGUST 17, 2022
BIOCHEMISTRY

[READ !\[\]\(c15650232aa6660c9deb34f3b82dcb72_img.jpg\)](#)

Comprehensive Transcriptomic Analysis of Novel Class I HDAC Proteolysis Targeting Chimeras (PROTACs)

India M. Baker, Shaun M. Cowley, *et al.*

AUGUST 10, 2022
BIOCHEMISTRY

[READ !\[\]\(06b7456efb47d301bca6298603e7f4fc_img.jpg\)](#)

[Get More Suggestions >](#)